Study of Structurally Induced Turbulence in Rotary Thermally Isolated Compressible Flow

By

Muhammad Zunair

Reg # 00000203670
Session 2017-2019

Supervised by
Dr. Majid Ali

A Thesis Submitted to the U.S.-Pakistan Centre for Advanced Studies in Energy in partial fulfillment of the requirements of the degree of

MASTER of SCIENCE
in
THERMAL ENERGY ENGINEERING

US-Pakistan Centre for Advanced Studies in Energy (USPCAS-E)
National University of Sciences and Technology (NUST)
H-12, Islamabad 44000, Pakistan

June 2021

THESIS ACCEPTANCE CERTIFICATE

Certified that final copy of MS thesis written by **Mr. Muhammad Zunair**, (Registration No. 00000203670), of U.S.-Pak Center for Advanced Studies in Energy has been vetted by undersigned, found complete in all respects as per NUST Statues/Regulations, is within similarities indices limit and accepted as partial fulfillment for award of MS/MPhil degree. It is further certified that necessary amendments as pointed out by GEC members of the scholar have also been incorporated in the said thesis.

Signature: _____

Name of Supervisor: Dr. Majid Ali

Date: _____

Signature (HoD): _____

Date: _____

Signature (Dean/Principal): _____

Date: _____

CERTIFICATE

This is to certify that work in this thesis has been carried out by **Mr. Muhammad Zunair** and completed under my supervision in, U.S.-Pak Center for Advanced Studies in Energy, National University of Sciences and Technology, H-12, Islamabad, Pakistan.

Supervisor: _____
Dr. Majid Ali
USPCAS-E, NUST H-12, Islamabad

GEC member 1: _____
Dr. Adeel Javed
USPCAS-E, NUST H-12, Islamabad

GEC member 2: _____
Dr. Adeel Waqas
USPCAS-E, NUST H-12, Islamabad

GEC member 3: _____
Dr. Ammar Mushtaq
RCMS, NUST H-12, Islamabad

HoD-TEE: _____
Dr. Adeel Javed
USPCAS-E, NUST H-12, Islamabad

Principal/Dean: _____
Dr. Adeel Waqas
USPCAS-E, NUST H-12, Islamabad

Acknowledgments

I am extremely thankful to **ALLAH Almighty** without Whose help I would not have been able to complete this work. All the help and support from my parents and teachers were only because of Allah's Will.

I am thankful to my supervisor, **Dr. Majid Ali**, for the tremendous supervision, motivation and guidance he has conveyed all through my time as his understudy. I have been exceptionally honored to have a supervisor who thought such a great amount about my work, and who responded to my inquiries and questions so immediately.

I am thankful to all GEC members and USPCAS-E for their support throughout the program. Finally, I am grateful for the National University of Sciences and Technology, Pakistan for providing research facilities in my work.

Regards,

Muhammad Zunair

Dedication

Dedicated to my beloved parents and all educated community who lead me to such tremendous and wonderful accomplishment and success

Abstract

Structurally induced turbulence in a fast-rotating gas was investigated by a CFD method. Turbulence induced in the flow field due to the interaction of fast rotating gas with collection structures was modeled with Reynold stress model (RSM). Finite volume method (FVM) with second order upwind scheme was used to solve the 3D Navier-Stroke's equation. Knudsen boundary was used to limit the computational domain in Iguassu Model. Effect of Multiple outlets and cylinder temperature gradient was also investigated. Simulation results showed the generation of three-dimensional shock waves propagating in axial direction along cylinder length. Wave intensity was increased, as the diameter of collection structure was increased. A radially inward flow was induced due to imbalance in pressure gradient and centrifugal force caused by the interaction of gas with collection structure. This inward flow significantly increased the countercurrent in axial direction. In case of two outlets, shielding baffle significantly decrease the turbulence effect due to one outlet in main chamber. Turbulence effect increases as the collection structure moves towards the cylinder wall. Countercurrent is also increased as a temperature gradient is applied on the cylinder wall. Increase in temperature gradient significantly increases the countercurrent.

Keywords: Knudsen boundary, Numerical methods, Rotating gas, Shock wave, Countercurrent

Table of Contents

List of Figures

Chapter 1

Introduction

High speed rotating gas is encountered in centrifuges. Centrifuge is a device, which is used to separate two fluids on the basis of their mass difference. Separation is achieved by rotating two fluids (with different mass) in a cylinder. Different centrifugal force act on both the fluids. Heavy fluid is pushed along the cylinder wall due to large centrifugal force while the relatively lighter fluid rotates at a shorter radius compared to the heavy fluid.

1.1. Areas of application

They have a very vast area of applications. At laboratory scale they are used to purify cells, separate blood cells, viruses, proteins and nucleic acids. At industrial level, they are used for separation of chlorine isotopes, enrichment of uranium and well gas separation[1].

1.2. Isotope separation

Centrifuges used for uranium enrichment separates two isotopes of uranium (molecular weight: 235kg/k-mol and 238kg/k-mol). Uranium hexafluoride gas (UF_6) is used for uranium isotopes separation. Gas entered the rotating cylinder through a center port. After entering the cylinder, gas is pushed to the cylinder walls leaving a high vacuum region in the cylinder center. Two structural elements are used to collect the two streams of gases, one enriched in U-238 (Waste) and other enriched in U-235 (Product) [2], [3].

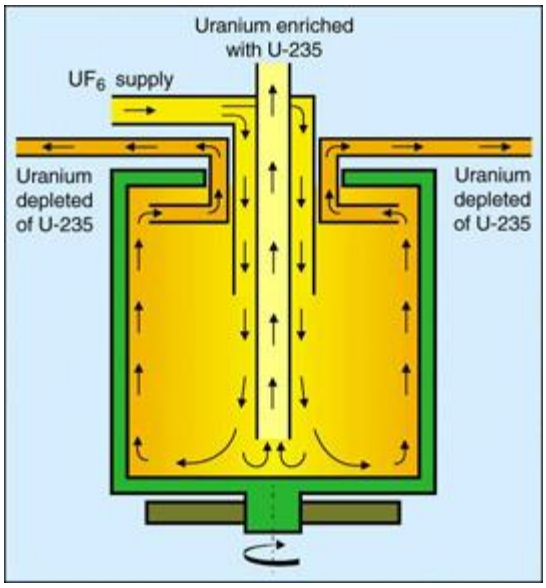

Figure 1.1 Flow in gas centrifuge [3]

1.3. Countercurrent

Separation occurred due to centrifugal force only, is very small. A countercurrent is generated in the rotating cylinder to increase the separation[4], [5]. This countercurrent is generated due to following factors,

1. Thermal profile of cylinder wall
2. Temperature difference on the cylinder ends
3. Feed inlet
4. Structure present in the cylinder to collect the waste and product

1.3.1. Effect of thermal drive on countercurrent

Thermal profile of cylinder wall facilitates the countercurrent when present in right direction. Cylinder wall end with high temperature increases the energy of gas molecules present near the wall and these molecules tends to move towards center (high vacuum region). This is analogous to the rise of a heated gas in atmosphere. When gas is heated it moves against the gravitational field. In rotating cylinder, dominant force field is centrifugal force field and when gas is heated, it

tends to move against the force i.e., towards the center. As heated gas moves towards the center, it sucked up in the vacuum towards the other end of the wall due to higher vacuum. On the other hand, as the heated gas moves towards the center, pressure drops near the wall and due to pressure difference, gas molecules from colder cylinder wall moves towards the lower pressure region along the wall. These two flows facilitate each other to generate a counter current in the rotating cylinder.

Temperature difference on cylinder ends effects the counter current in the same manner as cylinder thermal profile. Feed enters the cylinder in the center, starts rotating immediately and rapidly moves towards the cylinder wall. This motion of gas disturbs the counter current flow.

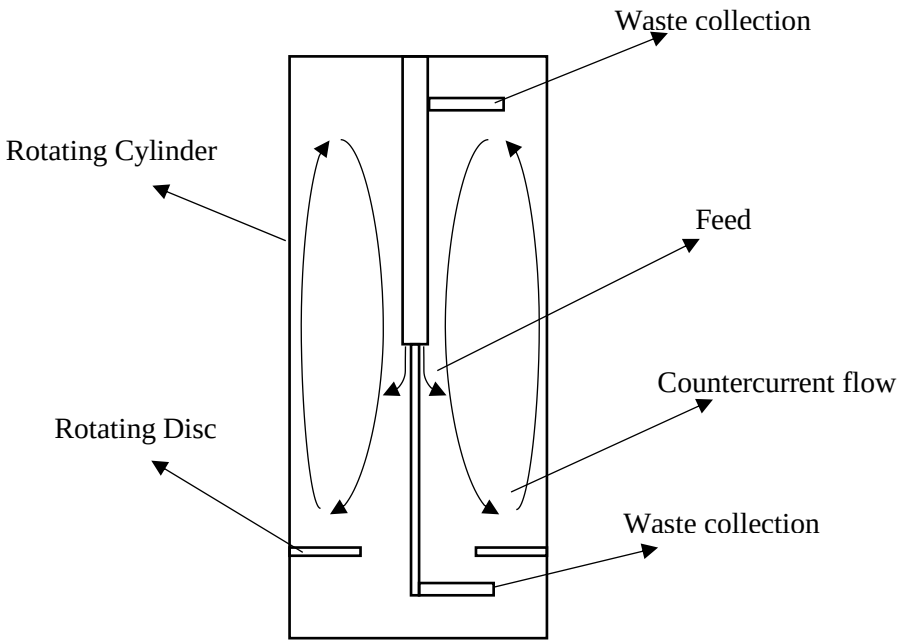

Figure 1.2: Schematic diagram of countercurrent in centrifuge

1.3.2. Effect of mechanical drive on countercurrent

Most important factor in the countercurrent is the presence of structural elements. Structural element disturbs the countercurrent in following three ways,

1. Heating of structure due to interaction of high-speed gas
2. Disturbance in flow due to physical presence of structure
3. Extraction of gas

Due to heating a thermal drive is introduced in the flow. Interaction of rotating gas with the structure produces a turbulence in the flow. This turbulence slows down the gas in its vicinity. This slowed down gas then sucked up in the central high vacuum core and cause a countercurrent in the cylinder. Extraction of gas creates a low-density region near the collection. Gas from surrounding region flow towards the structure to fill up the vacant region creating a net flow.

Two structural elements (for waste and product collection) are located at the opposite ends of cylinder along the cylinder length. Effect of both the structures on countercurrent opposes each other. To shield the effect of one structure, a disc is attached in the cylinder slightly above product collection. This disc rotates with the cylinder and prevents the turbulence produced, due to product collecting structure, entering the working zone of cylinder.

1.3.3. Turbulence due to waste collection structure

Turbulence produced in fluid due to presence of structural element in the working zone is very important parameter of design. Turbulence creates two opposing effects simultaneously, one favoring and other degrading the separation process. Turbulence causes the countercurrent in cylinder which increases the separation. It also increases mixing of streams in fluid domain near waste collection which disturbs the separation process. So, in order to properly design the location and size of waste collecting structure, we need to examine the turbulence produced in the fluid domain due to presence of structure.

1.4. Research problem

Axisymmetric model have been used previously to predict the turbulence[5], [6]. But as turbulence in rotating fluid due to structural element is of 3D nature, those results are far from actual[7]. So, a 3D model of rotating cylinder with structural elements is required to determine the three-dimensional effects of turbulence.

In this thesis, comprehensive model will be presented to determine the turbulence produced in a rotating cylinder due to presence of a structural element in the fluid stream. Effect of this turbulence on axial countercurrent flow will be examined. The effect of temperature gradient of cylinder wall on countercurrent will also be analyzed.

1.5. Research objectives

- To develop a CFD model in ANSYS Fluent for high-speed rotating fluid under the influence of centrifugal force
- To investigate the effect of turbulence on rotating flow field
- Determine the variation in density distribution along radial direction due to turbulence
- To investigate the effect of size and position of collection structure on turbulence
- To investigate the effect of temperature gradient on countercurrent

1.6. Thesis structure

Summary of different chapters in this thesis is as follow,

- **Chapter 2 Literature review**

It includes the different models proposed for high-speed rotating fluids, their limitations and evolution of models for analysis of different parameters affecting the flow regime.

- **Chapter 3 Computational model**

It includes methodology to build the model for fluid analysis, assumptions taken to build the model and limitation on computational domain

- **Chapter 4 Turbulence effect due to single outlet**

Effects of single outlet on flow regime is discussed in this chapter. Pressure and velocity profiles in rotating cylinder and generation of shockwaves due to structures are also discussed.

- **Chapter 5 Turbulence effect due to two outlets**

It includes the effect of two outlets on flow regime, effect of size and radial position of structure on turbulence and effect of shielding baffle on turbulence in main chamber.

- **Chapter 6 Effect of temperature gradient on countercurrent**

Effect cylinder temperature gradient on flow profile is discussed in this chapter. It also includes the effect of temperature gradient variation on single and two outlets.

- **Chapter 7 Conclusion and recommendations**

Conclusion drawn on the basis of different analysis are discussed in this chapter. Comparison with other models and future recommendations are also discussed.

1.7. Summary

High speed rotating cylinders are used for isotopes separation. During high-speed rotation, different centrifugal force acts on isotopes due to their mass difference. An axial countercurrent enhances the separation phenomenon. Collection structures present in flow regime of rotating fluid, produce turbulence. This turbulence increases the countercurrent flow and also cause the mixing of streams. To optimize the separation power of rotating cylinder, we need to optimize the turbulence. A model will be built to analyze and optimize the turbulence produced by the collection structure.

References

[1] "Centrifugation- Principle, Types and Applications | Instrumentation | Microbiology Notes." [Online]. Available: https://microbenotes.com/centrifugation-principle-types-and-applications/. [Accessed: 07-Aug-2019].

[2] "Gas centrifuge process." [Online]. Available: https://www.euronuclear.org/info/encyclopedia/g/gascentrifuge.htm. [Accessed: 07-Aug-2019].

[3] K. van Ommen, *Numerical modelling of a heavy gas in fast rotation*. 2010.

[4] D. A. De Andrade and J. L. F. Bastos, "Thermal hydrodynamical analysis of a countercurrent gas centrifuge," *Ann. Nucl. Energy*, vol. 25, no. 11, pp. 859–888, 1998.

[5] D. R. Olander, "The theory of uranium enrichment by the gas centrifuge," *Prog. Nucl. Energy*, vol. 8, no. 1, pp. 1–33, 1981.

[6] W. Nakayama and S. Usui, "Flow in rotating cylinder of a gas centrifuge," *J. Nucl. Sci. Technol.*, vol. 11, no. 6, pp. 242–262, 1974.

[7] V. D. Borman, S. V. Bogovalov, V. D. Borisevich, I. V. Tronin, and V. N. Tronin, "The computer simulation of 3d gas dynamics in a gas centrifuge," *J. Phys. Conf. Ser.*, vol. 751, no. 1, 2016.

Chapter 2

Literature Review

Over the year, different methods have been adopted by scientists and researchers to model flow in rotating cylinder. Conventional codes to solve Navier-Stroke's equation were not applicable in this case as due to strong centrifugal force, unrealistic mass flow values were obtained at the interfaces of control volume. The axial countercurrent mass flow was very small (of the order of centimeter or even millimeter per second). Density and pressure vary strongly along radial direction and collection structure had very complex shape so customized codes had been developed to solve these equations for gas field [1].

Initial attempts to solve the model had many assumptions to simplify the model. Rotating cylinder was considered very long to neglect the effect of end plates [2]. Thermal and mechanical drives of countercurrent were usually considered alternately to study their effects [3]. Collection structure had been modeled differently by many researchers to correctly model their effects [4], [5], [6]. Onsager presented first comprehensive model to study the flow in rotating cylinder [4].

Initially 2D asymmetrical models were used due to lack of computations power. With the evolution, as computation power was increased, more complex 3D transient models evolved and overcame the limitation of 2D models. Different methods which had been used to solve the model are described below,

2.1. Coriolis effect

In 1974, Wataru NAKAYAMA and Sampei USUI formed a model to incorporate the effect of Coriolis force in the rotating fluid [3]. Scaling analysis was made to determine the dominance of Coriolis force in different regions of

rotating cylinder. Model was based on following assumptions to simplify the model,

1. Centrifugal acceleration was very large so gravitational effects have been neglected
2. Rotating gas was assumed as a perfect gas
3. Thermally conductive walls of rotating cylinder have been assumed
4. Gas properties like viscosity, thermal conductivity and specific heat were assumed constant
5. Density variation along the cylinder axis were neglected

To determine the flow pattern, feeding and discharging ports have been considered and inlet and outlets were provided through the top and bottom part of cylinder i.e. no inlet or outlet was considered near the rotor wall. Central region was treated as inviscid region while viscous boundary layers were considered near the cylinder wall.

Results showed that scaling analysis supported the dominance of Coriolis force in whole flow field except in central region of ultrahigh speed cylinders. Thermal gradient on cylinder wall directly affects the convection in viscous boundary layer near the cylinder wall.

2.2. Onsager's model

Onsager's model presented a comprehensive CFD model of high-speed rotating fluid. He linearized the conservation equations of mass, momentum and energy. Onsager combined these equations to give a single six order linearized differential equation (Appendix A) which described the counter current flow in Stewartson layer. Equations were solved using eigen function expansion method. He modeled the collection structure as source of heat due to friction and sink of momentum due to drag produced by the structure [4]. Boundary conditions used to solve the Onsager's equations were as follow,

- No slip condition was considered at cylinder wall
- Radial component of velocity u vanishes along the wall

- Temperature distribution along the cylinder wall was given by a quadratic function
- Onsager simplified the model by neglecting the inner core with very small amount of gas and defined an inner boundary at a radial distance where the corresponding distance on unit scale is equal to the mean free path length of gas molecule (Appendix B)
- Flow enters in radial direction at Stewartson layer
- Axial velocity had no radial gradient at inner layer
- Radial gradient of temperature and azimuthal velocity perturbation were assumed to vanish at inner wall of fluid flow

He proposed that there are four mechanisms which cause the counter current in high-speed rotating cylinder,

1. Wall thermal drive
2. End cap thermal drive
3. Scoop drive
4. Feed drive

Onsager proposed two types of parameters (External and internal), based on his master equation, to optimize the flow in rotating cylinder. External parameters of flow are throughput (Inflow mass flow rate) and cut (Ratio of mass flow rates of waste and product outlet), while Internal parameters includes,

1. Temperature gradient on cylinder wall
2. Temperature difference between cylinder end caps and gas present at the ends of cylinder
3. Radial position of waste and product collection structure
4. Size of tip of waste and product collection structure
5. Density of rotating gas at cylinder wall
6. Axial position of feed inlet

2.3. Countercurrent flow modeling

To solve the countercurrent flow in a rotating cylinder, L. D. Cloutman and R. A. Gentry proposed an asymmetrical model in 1983. Finite difference method with time-marching approach was applied to solve the linearized Navier-Stroke's equations [7].

Feed and structural effects in rotating gas field were modeled as source terms. Implicit diffusion terms were used to cater the large density variation along the radial direction in rotating cylinder. To capture the thin boundary layer along the cylinder wall and cylinder ends, a nonuniform mesh grid with fictional mesh layers was used.

2.4. Effect of thermal drive on countercurrent

To analyze the effect of thermal drive on countercurrent flow, Andrade and Bastos proposed a steady state axial symmetrical model using Navier-Stroke's equation in cylindrical coordinate system (Appendix C) [5].

Flow was assumed as laminar and compressible. Constant physical properties were assumed. Collection structure was modeled with a disc having 10% less rotational speed than the cylinder. Model was solved using Finite Volume Method with SIMPLE technique. Main heat sources considered in the model were, induction motor, axial bearing, gas coming in contact with structural element and molecular vacuum pump. Convection and radiation heat transfers were also taken account in the model.

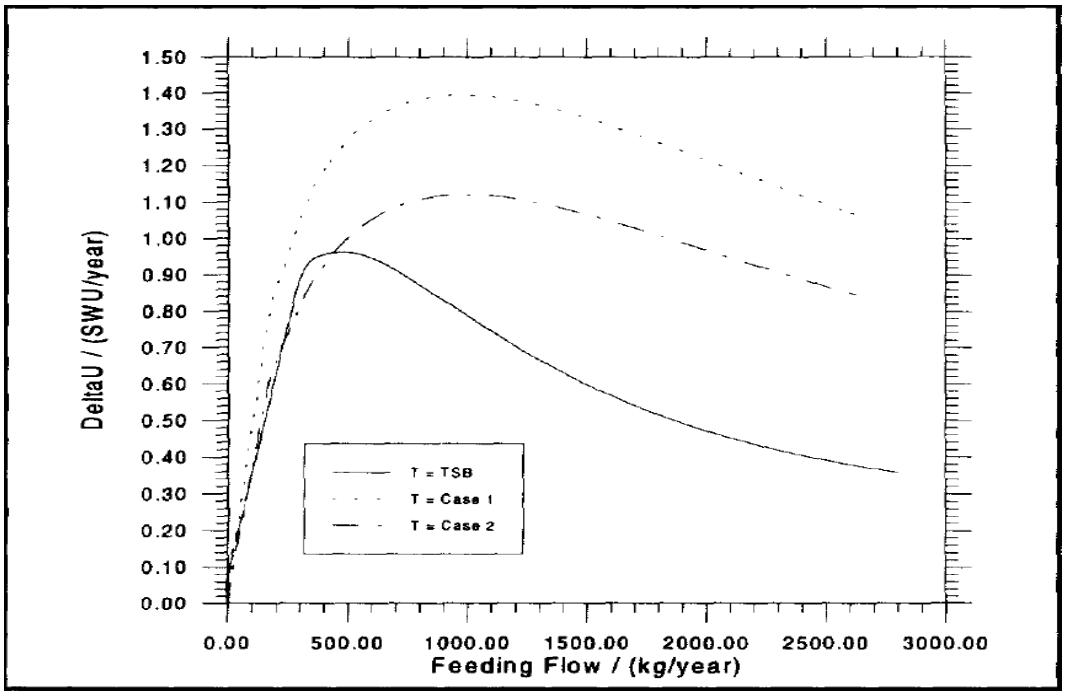

Figure 2.1: Separative power with different thermal boundary conditions [5]

Three different cases were examined to understand the effect of thermal drive, Case1 with same cylinder wall temperature showed very small separative power. Case 2 was presented with cylinder having 23^{o}C temperature gradient along its wall. It showed the highest separative power. Case 3 used material with different optical properties to optimize the heat transfer during cylinder rotation. Same cylinder wall temperature was used and it showed a moderate separative power.

2.5. Numerical solution of Onsager's pancake model

M. de Stadler and K. Chand solved Onsager's master equation numerically to simulate the flow model in rotating cylinder [2].

Axisymmetric incompressible subsonic flow was modeled using cylinder as a long rotating cylinder. He derived a semi analytic, grid independent solution of Onsager's equation. Overture software was used to solve the system of differential equations with total reflux condition (No mass in or out). No wall thermal drive or mechanical drive due to collection structure were considered.

2.6. 3D CFD model

Jiang et al. solved 3D Navier-Stroke's equation using vector splitting method of finite volume method. Implicit second order scheme was used and effect of wall temperature and feed flow were neglected in the model. Cylinder, baffle and top and bottom plates of cylinder were modeled as rotating walls while collection structure was modeled as stationary wall [8].

Results indicated production of a shock wave in working chamber in front of stationary structure. Wave became stronger as the radial length of structure increases. An oblique shock wave between structure and cylinder caused a pressure increase on cylinder wall and caused an inward flow of gas due to unbalance of centrifugal force and pressure gradient.

2.7. Bogovalov's 3D model

Bogovalov et al. proposed a 3D CFD model to analyze effect of different parameters on rotating flow field. He studied different cases by varying different parameters in flow field to study their effects.

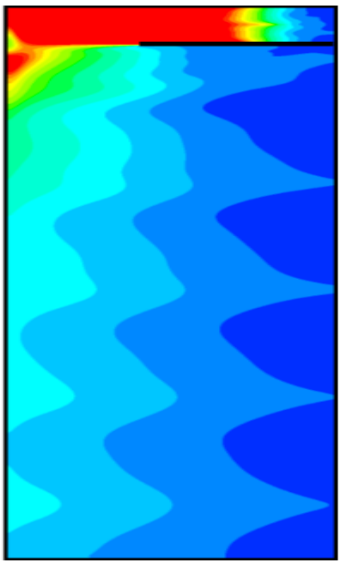

Figure 2.2: Wave generation [10]

2.8. Model to study the waves propagation in flow field

When gas rotating at high speed come in contact with a structural element, three kinds of waves are generated which propagates along the cylinder axis. S.V. Bogovalov et al. solved the Linearized axisymmetric 3D Navier-Stroke's equation in transient state to form a model to investigate these waves [9], [10].

Instead of defining the Knudsen boundary, he used whole domain to apply his model. Effects of viscosity and thermal conductivity were also neglected.

Results showed presence of three types of wave families. Two types of wave are present in rarefied gas region and damped quickly while the third type is present in dense region and propagates longer than the other two.

2.9. Model to study impact of pulsed breaking force on flow field

Collection structures were modeled as sources of mass, momentum and energy. Following two cases were studied for this model,

1. Conventional steady state source
2. Pulsed source of momentum and energy

Computational domain was limited at Knudsen number =10. Effects of feed, waste and product mass flow rates on flow field were neglected. Isothermal Cylinder wall condition was assumed. Countercurrent mass flux in stationary case was almost half the mass flux in pulsating source case [6].

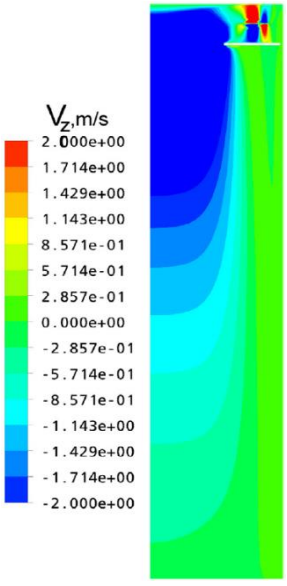

Figure 2.3: Axial velocity in working camera of GC in stationary case [6]

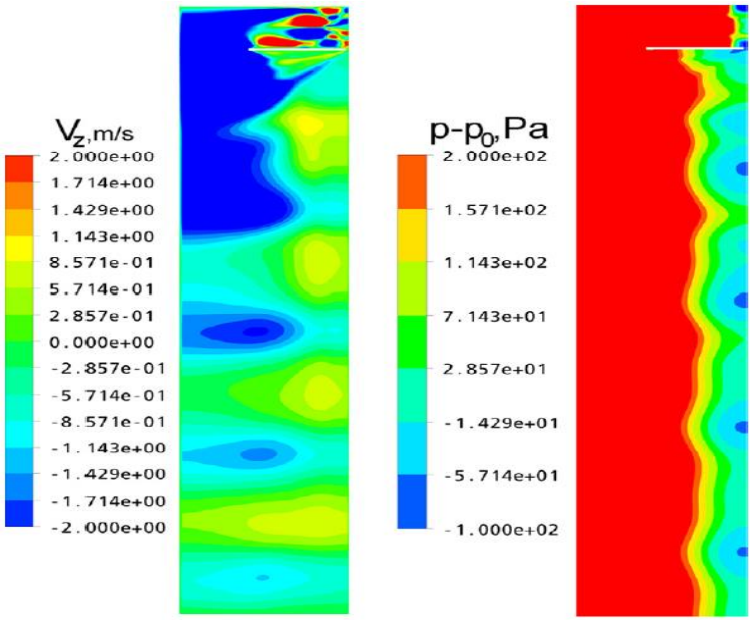

Figure 2.4: Axial velocity and pressure difference in the working camera with pulsed breaking force [6]

2.10. Model to study the effect of transient condition on flow field

Both transient and steady state cases were simulated. Computational domain was limited at Knudsen number =10. Effects of feed mass flow rate on flow field was neglected. 10K temperature gradient of cylinder wall was

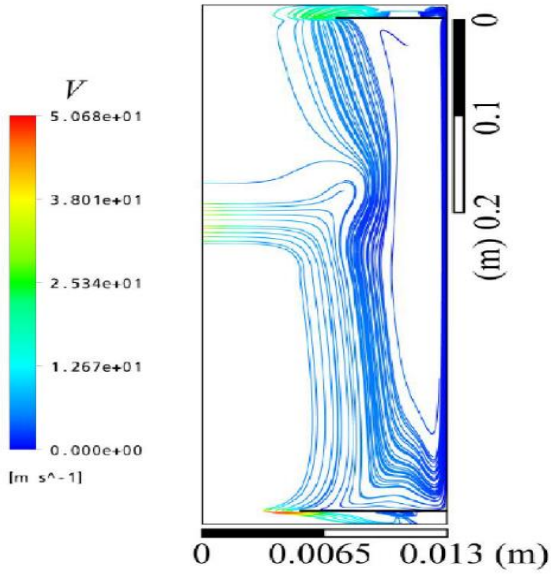

Figure 2.5: The stream line in the case of the stationary braking force [11]

considered. Pressure in product chamber and consequently product flux in steady state case is approximately 15% less as compared to transient state [11].

2.10. Model to study the deviation of 2D model from actual values

Model was solved as a steady state problem. Collection structures were modeled as wall with no slip condition. Computational domain was limited at Knudsen number =1. Effects of feed mass flow rate on flow field was neglected. Mass flow inlet was assumed at waste collection structure. Pressure outlet was assumed at Product collection structure. Temperature gradient of cylinder wall was considered. 2D model deviates 20-30% from real parameters due to 3D character of flow [1].

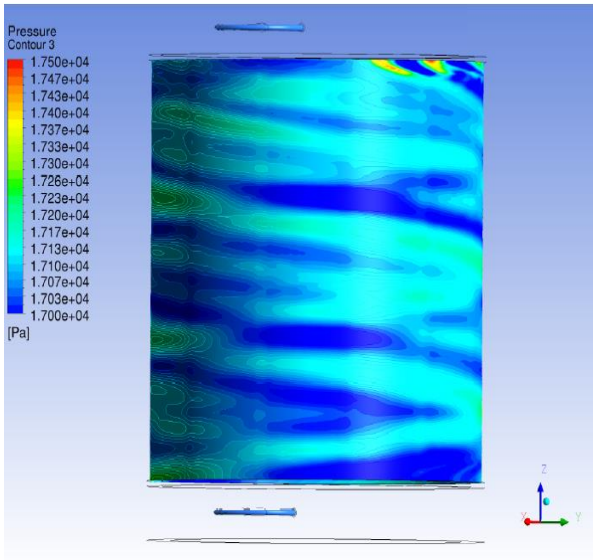

Figure 2.6: Variation of the pressure in the working chamber produced by the waves [1]

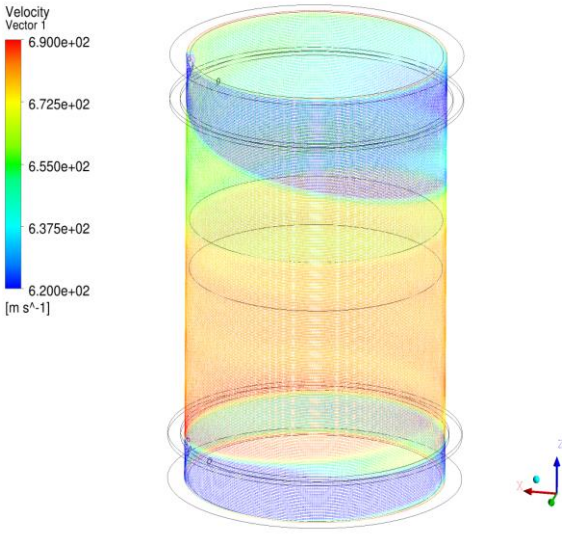

Figure 2.7: Velocity distribution on a cylindrical surface located in the computational domain [1]

2.11. Effect of feed on rotating gaseous flow field

To investigate the effect of feed jet on rotating gas field, a 3D CFD model was used. Finite volume method with second order implicit upwind scheme was

used to solve the model. Realizable turbulence model was used to capture the turbulence effect. Inlet boundary condition was mass flow inlet. Outlet boundary condition was Pressure outlet. Computational domain was defined on the basic of Knudsen number. Constant cylinder wall temperature was considered. Velocity in axial and radial direction was also neglected[12].

Affected gas flow region due to feed inlet was very small. As gas entered the cylinder, it rapidly moved towards the cylinder wall due to high pressure gradient and loss of axial momentum so the effect of feed on the flow was very limited.

2.12. Summary

To study the effects of different parameters on flow field of a rotating gas, different models have been developed. No single model has been developed yet which can completely define gaseous flow field in high-speed rotation. Collection structure has been modeled in many different ways to study its effect on flow field. Turbulence effects are much more significantly captured when 3D model is considered. Turbulence effects are significant in high gas density regions (near the cylinder wall), these effects vanish as we move in less dense region i.e. towards the axis of rotation in radial direction.

References

[1] V. D. Borman, S. V. Bogovalov, V. D. Borisevich, I. V. Tronin, and V. N. Tronin, “The computer simulation of 3d gas dynamics in a gas centrifuge,” *J. Phys. Conf. Ser.*, vol. 751, no. 1, 2016.

[2] M. De Stadler and K. Chand, “A Finite-Difference Numerical Method for Onsager ’ s Pancake Approximation for Fluid Flow in a Gas Centrifuge,” 2007.

[3] W. Nakayama and S. Usui, “Flow in rotating cylinder of a gas centrifuge,” *J. Nucl. Sci. Technol.*, vol. 11, no. 6, pp. 242–262, 1974.

[4] D. R. Olander, “The theory of uranium enrichment by the gas centrifuge,” *Prog. Nucl. Energy*, vol. 8, no. 1, pp. 1–33, 1981.

[5] D. A. De Andrade and J. L. F. Bastos, “Thermal hydrodynamical analysis of a countercurrent gas centrifuge,” *Ann. Nucl. Energy*, vol. 25, no. 11, pp. 859–888, 1998.

[6] S. V. Bogovalov, V. A. Kislov, and I. V. Tronin, “Impact of the pulsed braking force on the axial circulation in a gas centrifuge,” *Appl. Math. Comput.*, vol. 272, pp. 670–675, 2016.

[7] “Numerical Simulation of the Countercurrent Flow in a Gas Centrifuge Los Alamos National Laboratory Los Alamos , New Mexico 87545,” no. March, 1983.

[8] D. Jiang and S. Zeng, “CFD Simulation of 3D Flow field in a Gas Centrifuge,” *Int. Conf. Nucl. Eng. Proceedings, ICONE*, vol. 2006, 2006.

[9] S. V. Bogovalov, V. A. Kislov, and I. V. Tronin, “Waves in strong centrifugal fields: dissipationless gas,” *Theor. Comput. Fluid Dyn.*, vol. 29, no. 1–2, pp. 111–125, 2015.

[10] S. V. Bogovalov, V. A. Kislov, and I. V. Tronin, “Gas dynamics in strong centrifugal fields,” *AIP Conf. Proc.*, vol. 1648, no. March 2017, 2015.

[11] S. V. Bogovalov, V. A. Kislov, and I. V. Tronin, “Waves in a gas centrifuge,” *J. Phys. Conf. Ser.*, vol. 751, no. 1, 2016.

[12] D. J. Jiang and S. Zeng, “3D numerical study of a feed jet in a rotating flow-field,” *J. Phys. Conf. Ser.*, vol. 751, no. 1, pp. 6–11, 2016.

Chapter 3

Computational Model

This thesis is based on modeling of gas flow in a rotating cylinder in the presence of collection structures. Navier strokes equations were used to model the system (Appendix C). To simplify the model effect of temperature variation in fluid properties (Specific heat, thermal conductivity, viscosity) was assumed to be very small and hence neglected in the calculation.

Gas enters the cylinder from center and rapidly moves towards the cylinder wall due to high centrifugal force. So, most of the gas is present in the region near cylinder wall and high vacuum region exists in cylinder center. We are concerned only with the gas region and our computational model is not valid in vacuum so we limited our computational domain by Knudsen number. Computational model is valid only in the region where Knudsen number is less than 10.

Knudsen number is calculated through following method [1],

$$K_n = \frac{\lambda}{R} \tag{3.1}$$

Here,

$R =$ Radius of rotating cylinder, $\lambda =$ Mean free path length

Mean free path length is calculated through following formulation,

Mean Free Path Length: $$\lambda = \frac{M}{\sqrt{2}\pi\sigma^2\rho_o N_{av}} \tag{3.2}$$

Here

$N_{av} = Avogadro\ number$, $\sigma =$ Molecular diameter of gas,

$\rho_o =$ density of gas, M = Molecular weight of gas

$$\rho_o = \rho_w e^{-A^2\left[1-\frac{r^2}{a^2}\right]} \quad (3.3)$$

$$A^2 = \frac{M\sigma^2 a^2}{2RT_o} \quad (3.4)$$

Ωa= Peripheral speed, r= Cylinder Radius

A program file was formed in Microsoft Excel to calculate the Knudsen boundary. Knudsen boundary in our case was calculated to be located at a radius of 0.056m.

Navier-Stroke's equation in 3D cylindrical coordinate system for steady state were solved through a commercially available software (ANSYS Fluent).

3.1. Geometric model

3D geometric model was built in Solid Edge. To study the 3D nature of flow, curved collection structures are used in the simulation. Iguassu model was used with following parameters[2],

$Radius\ of\ rotating\ cylinder = 0.065m$

$Length\ of\ rotating\ cylinder = 0.224m$

$Collection\ structure\ diameter = 0.0075m$

$Distance\ of\ collection\ structure\ from\ cylinder\ top = 0.0175m$

3.2. Computational grid

A structured mesh was generated in ANSYS ICEM. Mesh quality was maintained above 0.5. Mesh is refined near collection structure and fine radial layers were added to capture the shock waves near cylinder wall region.

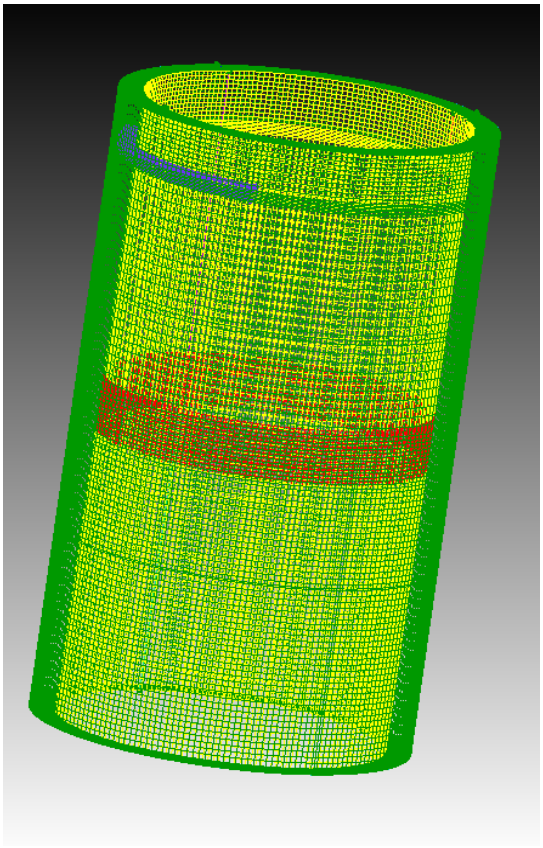

Figure 3.1: Grid generation of computational domain

Grid independency test was performed with gas pressure at rotor wall to optimize the number of elements and element size in the grid. As the results become constant after approximately 500000 elements. So, we choose 565957 total elements for our calculation.

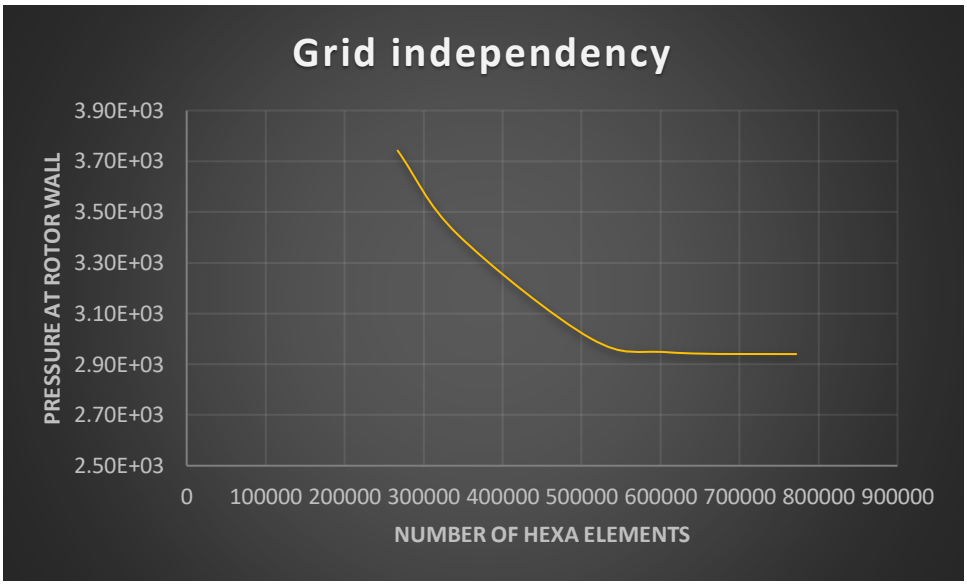

Figure 3.2: Grid independency

3.3. Ansys model

Ansys Fluent was used for solution of the problem. Pressure-based solver with steady state condition is used. Operating pressure was assigned a value of 0pa. Effect of gravity was neglected due to presence of strong centrifugal force.

3.3.1. Turbulence model

Reynold stress 7 equation model [3] was used for turbulence modeling of problem due to following reasons,

- RSM accounted for the effects of streamline curvature, swirl, rotation, and rapid changes in strain rate
- It had strong coupling between Reynolds stresses and mean flow
- It was recommended for cyclones and high-speed swirling flows
- Low computational resources restricted the use of LES turbulence model

As our flow was swirling and in curved path so we used Stress-Omega model with compressibility effects and viscous heating. Turbulence parameters were calculated as follow,

$$Turbulent\ Kinetic\ energy = k = \frac{3(u_{avg}I)^2}{2} \quad (3.5)$$

$$Specific\ dissipation\ rate = \omega = \frac{k^{\frac{1}{2}}}{c_u l} \quad (3.6)$$

$$Turbulent\ dissipation\ rate = \epsilon = \frac{k^{\frac{3}{2}}}{l} \quad (3.7)$$

$$Turbulent\ viscocity\ ratio = \frac{u_t}{u} = \frac{\rho c_u k^2}{\epsilon \mu} \quad (3.8)$$

Here,

$c_u = Empirical\ Constant = 0.09$

$$\upsilon = Turbulent\ viscocity = c_u \sqrt{\frac{3}{2}} \frac{u_{avg}}{l} \quad (3.9)$$

All properties were calculated for each case through a program file formed in Microsoft Excel.

3.3.2. Gas properties

User defined gas (UF6) was modeled as compressible ideal gas with following properties [4],

$$Molecular\ Weight = M = 352 \frac{kg}{kmol}$$

$$Viscosity\ of\ gas = \upsilon = 1.83E^{-05}\ Pa.s$$

$$Specific\ heat = C_p = 0.385 \frac{kJ}{kg.K}$$

$$Thermal\ Conductivity = \lambda = 0.0061 \frac{\mathrm{W}}{m.K}$$

$$Specific\ Heat\ Ratio = \gamma = \frac{C_p}{C_v} = 1.067$$

$$Gas\ constant = R = 23.62 \frac{J}{kg.K}$$

$$Speed\ of\ sound\ in\ gas\ at\ 300K = \sqrt{\gamma RT} = 86.95 m/s$$

3.3.3. Boundary conditions

- Mass flow inlet and pressure outlet were used as boundary conditions. Mass inlet value of $2 \times 10^{-05} kg/s$ was used for calculation with pressure outlet value of 2000Pa
- Gas entered the cylinder at constant temperature of 300K
- Cylinder was modeled as rotating wall with constant temperature value of 300K having following rotational speed (Iguassu model[5])

$$Rotational\ Speed = \omega = 2\pi \times 1700 s^{-1}$$

- No slip condition was applied on cylinder while the Knudsen boundary was modeled with free slip condition
- Collection structures were modeled as stationary walls with no heat flux.

3.3.4. Pressure velocity coupling

Problem was steady state and involves turbulence, so we used SIMPLE scheme. Second order upwind scheme was used for spatial discretization of all variables.

3.4. Solution strategy

Hybrid initialization with specified inlet pressure was used. Solution was started with small under relaxation values (as follow) and 10% of actual rotational speed,

$$Under\ relaxation\ factor\ for\ pressure = 0.3$$

$Under\ relaxation\ factor\ for\ density = 1$

$Under\ relaxation\ factor\ for\ body\ force = 1$

$Under\ relaxation\ factor\ for\ momentum = 0.5$

$Under\ relaxation\ factor\ for\ specific\ dissipation\ rate = 0.5$

$Under\ relaxation\ factor\ for\ turbulent\ viscosity = 0.5$

$Under\ relaxation\ factor\ for\ turbulent\ Reynold\ stresses = 0.3$

$Under\ relaxation\ factor\ for\ turbulent\ viscosity = 1$

As solution started to converge, rotational speed was increased to its original value and under relaxation values are returned to their original value.

3.5. Summary

Ansys Fluent was used for flow modeling in rotating cylinder. Geometry generated in Solid-Edge was imported in ICEM (Ansys) for mesh generation. Computational domain was limited by Knudsen boundary. RSM was used for turbulence modeling. Customized working gas was used for flow modeling and Iguassu model was used for boundary conditions and other computational parameters.

References

[1] D. R. Olander, “The theory of uranium enrichment by the gas centrifuge,” *Prog. Nucl. Energy*, vol. 8, no. 1, pp. 1–33, 1981.

[2] S. M. Romanihin and I. V Tronin, “Determination of the optimal mesh parameters for Iguassu centrifuge flow and separation calculations,” *J. Phys. Conf. Ser.*, vol. 751, p. 012007, 2016.

[3] T. Model *et al.*, “Chapter 10. Modeling Turbulence,” 2001.

[4] K. van Ommen, *Numerical modelling of a heavy gas in fast rotation*. 2010.

[5] S. V. Bogovalov, V. A. Kislov, and I. V. Tronin, “Waves in strong centrifugal fields: dissipationless gas,” *Theor. Comput. Fluid Dyn.*, vol. 29, no. 1–2, pp. 111–125, 2015.

Chapter 4

Turbulence due to single outlet

In first case, we took one outlet located at the top side of cylinder. Outlet structure diameter was set to 0.006m. Structure was located at 0.015m from top surface of cylinder and 0.035m from cylinder wall. Pressure outlet was used as boundary condition with 2000Pa gauge pressure.

4.1. Pressure profile

Results showed that the most of the gas was present near the cylinder wall region due to high centrifugal force. This caused high pressure values near cylinder wall and high velocity of gas molecules along cylinder wall as shown in Figure (4.1,4.2).

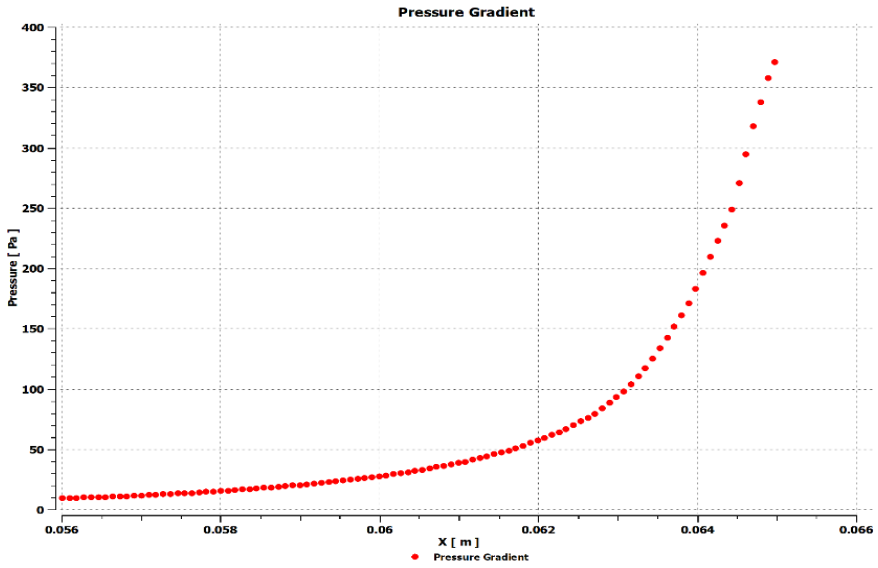

Figure 4.1: Pressure distribution along radial direction

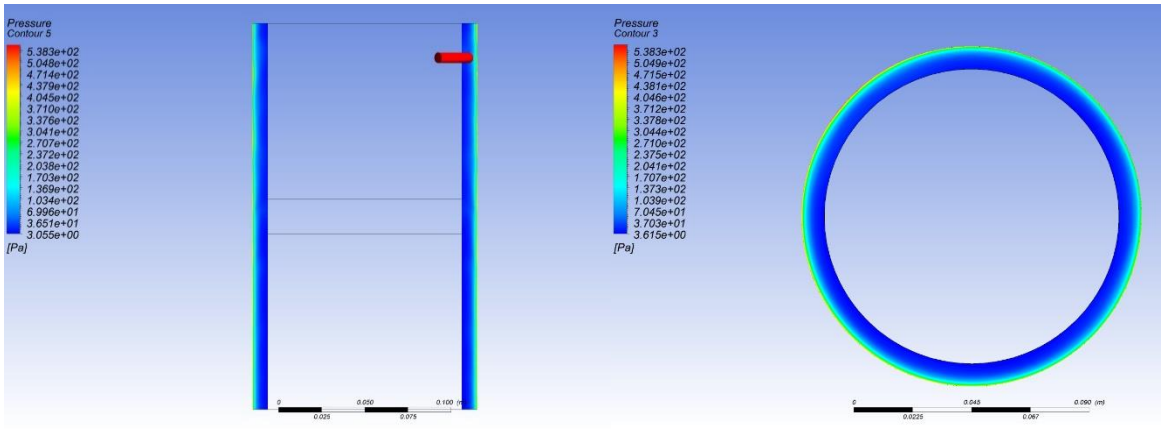

Figure 4.2: Pressure profile of rotating cylinder

As high-speed gas came in contact with the structure, shock waves were generated and they traveled in axial direction along the cylinder length.

These waves disturbed the pressure distribution in axial direction. These spiral waves were the produced near the outlet structure and lost intensity as they moved away from the structure (Figure 4.3).

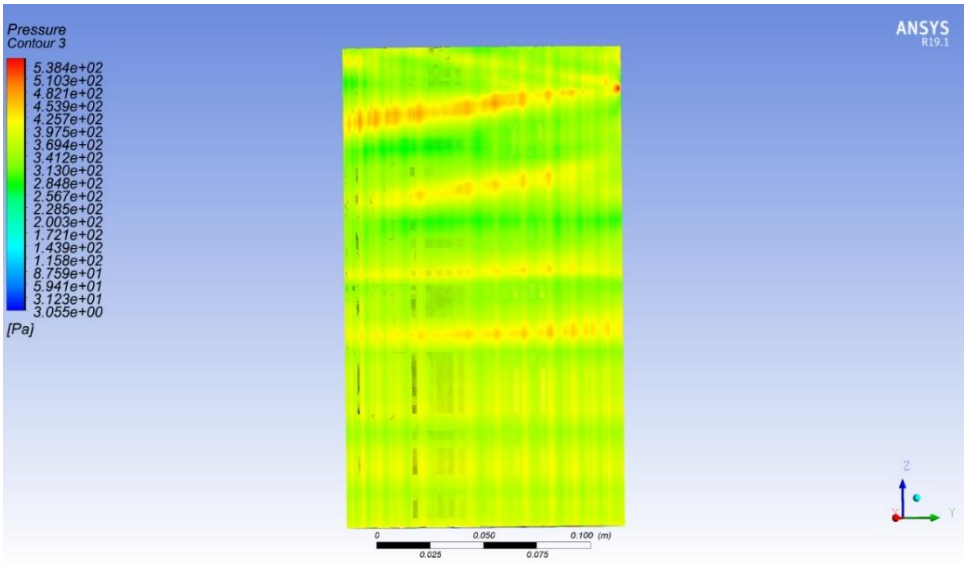

Figure 4.3: Spiral waves in axial direction

4.2. Velocity profile

Velocity profile of rotating cylinder showed that high velocity values were achieved by the gas near cylinder wall due to no slip condition on cylinder wall. Velocity near the collection structure was reduced due to stationary outlet structure (Figure 4.4,4.5).

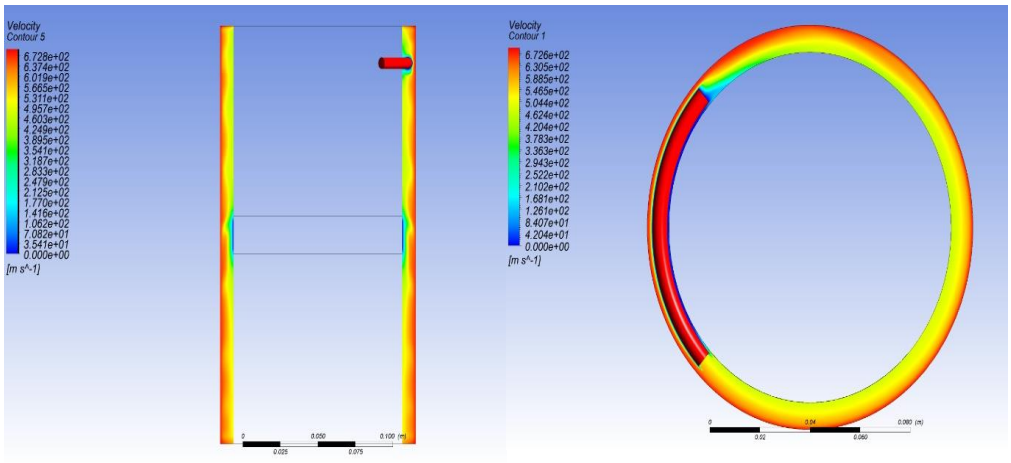

Figure 4.4: Velocity Profile of rotating cylinder

Axial velocity profile (Figure 4.5) showed the propagation of spiral shockwave in axial direction. These waves were 3D in nature and were the main cause of countercurrent flow. Intensity of these waves decreased as they moved towards the bottom of cylinder.

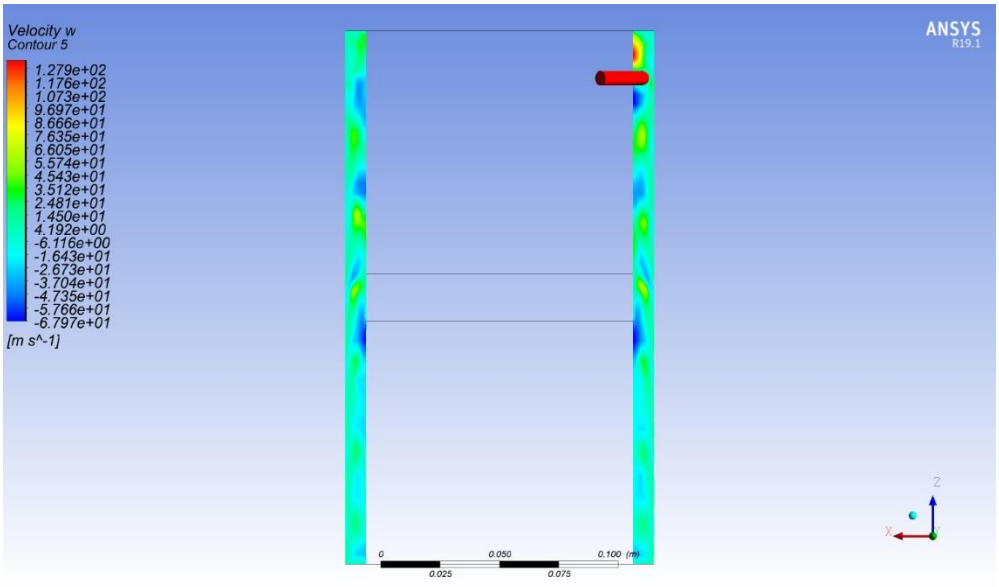

Figure 4.5: Propagation of shock waves in axial direction

4.3. Shockwave propagation

Shockwave propagation in gas was governed by following equation,

$$\omega = kc \tag{4.1}$$

Here

$\omega = rotational\ speed$

$k = wavenumber = \frac{2\pi}{\lambda}$

$\lambda = wavelength\ of\ wave$

$c = speed\ of\ sound\ in\ concerned\ madium$

Speed of sound in gas is calculated as follow,

$$c = \sqrt{\frac{\gamma RT}{M}} \tag{4.2}$$

Here,

$\gamma = Specific\ heat\ ratio = 1.067$

$R = Universal\ gas\ constant = 8314 \frac{J}{kmol.K}$

T= Average gas temperature = 300K

$M = Molecular\ weight\ of\ the\ gas = \ 352 \frac{kg}{kmol}$

Speed of sound calculated in our case was 87m/s and rotational speed was 10680rad/s. So, the wavelength of the shockwave with dispersion law was 50mm.

Wavelength of the shockwaves captured in our simulation was measured to be approximatly 45mm, which was in close approximation with the calculated value. This result showed that generation and propagation of shockwaves in rotating cylinder could be modeled with the wave dispersion law.

4.4. Summary

Pressure and velocity profiles were examined in the rotating cylinder. A strong radial pressure gradient was existed in flow. Obstruction in flow field due to collection structure caused the generation of shockwaves. Propagation of these shock waves were observed to follow the gas dispersion law.

References

[1] S. V. Bogovalov, V. A. Kislov, and I. V. Tronin, “Waves in a gas centrifuge,” *J. Phys. Conf. Ser.*, vol. 751, no. 1, 2016.

Chapter 5
Turbulence Due to Two Outlets

In this case we considered two outlet structures. Flow enters through center and collected through two structurers located near top and bottom surface of cylinder. Both structures were located at different distances from cylinder wall.

Top side structure was 3mm in diameter and located at 10mm from top surface of cylinder and 3mm away from cylinder wall. Bottom structure was 2mm in diameter and located at 5.3mm from bottom side of cylinder and 1.8mm from cylinder wall. Pressure outlet of 2000Pa was used as boundary condition at both outlet structures.

5.1. Velocity and pressure profile

A strong pressure gradient was available along radial direction as in the case of single outlet but in this case the bottom structure is located relatively near the cylinder wall and causing disturbance in pressure profile in radial as well as axial direction. Presence of bottom structure in relatively higher-pressure region was causing the gas molecules to slow down near the structure and caused strong counter current in axial direction.

Velocity vectors across the bottom collection structure showed that the flow was relatively smooth along the outlet face of structure. Flow disturbance was caused along the blunt face of the structure. So, to avoid this flow disturbance, non-collection end of the structure should be more aerodynamically smooth.

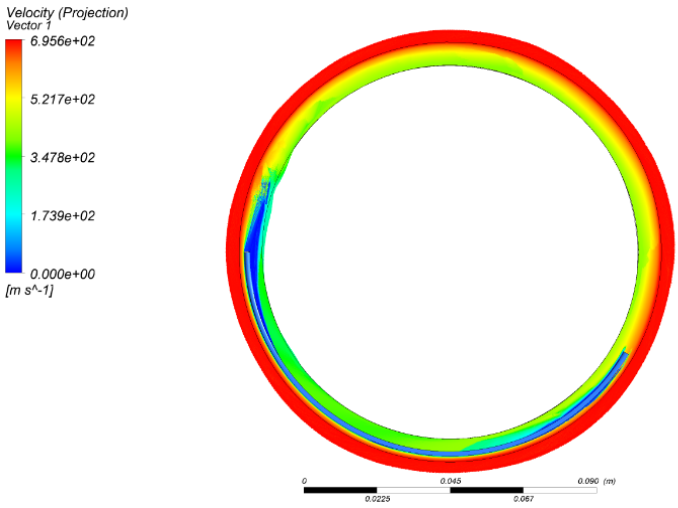

Figure 5.1Tangential velocity vectors

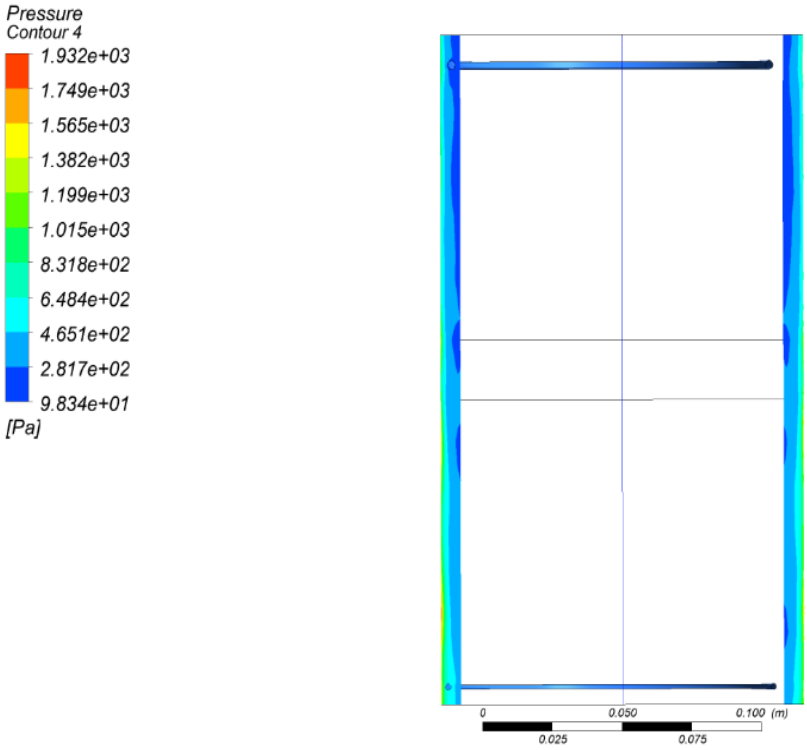

Figure 5.2: Pressure Profile with two outlets

Shockwaves are also generated near collection structures in this case as well and propagated in axial direction. Shockwave intensity was higher near the bottom structure indicating the more severe effects as distance between collection

structure and cylinder wall was decreased. Wavelength of wave was measured to be 53mm which was in close approximation to the calculated value of 50mm from wave dispersion law (Chapter 4).

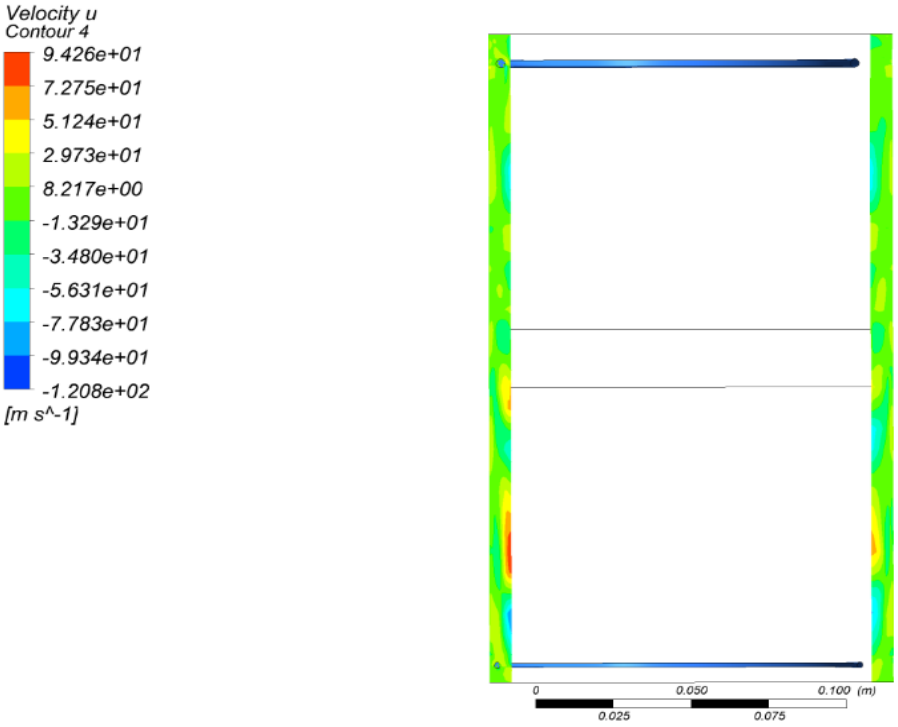

Figure 5.3: Velocity profile with two outlets

Turbulence effects in the flow field due to bottom structure were more severe than the top structure due to high pressure near cylinder wall. This effect disturbed the flow profile in central flow region and need to be minimized to achieve a constant flow profile in cylinder center.

A shielding baffle above the bottom structure was added to prevent the propagation of turbulence effect due to bottom structure in axially upward direction. Shielding baffle was added as a part of cylinder so it had same boundary condition as the cylinder i.e., rotating wall with rotational speed of $2\pi \times 1700 s^{-1}$ (Chapter 3). Physical dimensions of shielding baffle were as follow,

$Baffle\ ID = 0.0059m$

$Axial\ distance\ of\ baffle\ from\ bottom\ surface\ of\ cylinder = 0.01m$

5.2. Shielding baffle effect

Axial velocity profile of rotating cylinder with shielding baffle showed that the intensity of shock wave was reduced and turbulence effects were contained below the baffle. Pressure profile was smoother in the center region and high-pressure values were achieved behind the bottom structure below the baffle.

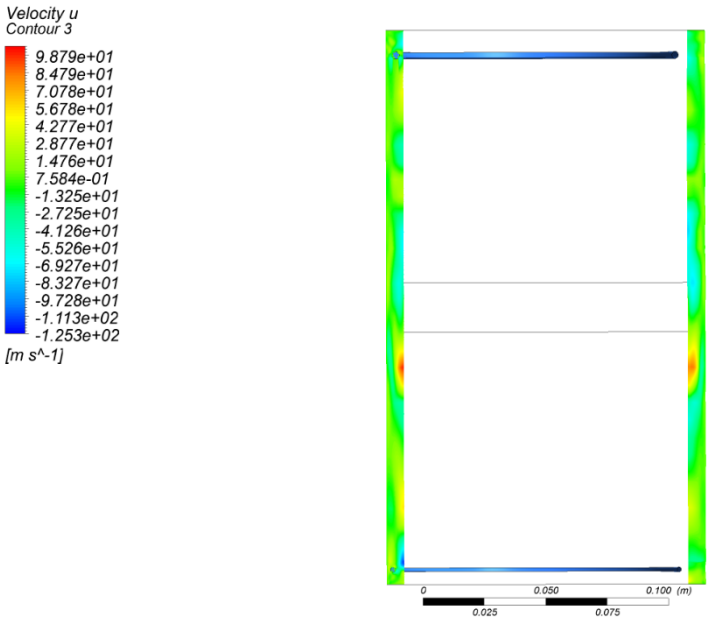

Figure 5.4: Axial velocity with shielding baffle

Presence of velocity gradient near the knudsen boundary showed that the due to obstruction of flow field, gas molecules actually entered the central high vacuumed region which we have ignored in our modeling. Countercurrent responsible for axial flow, actually exchanged gas molecules with central high vacuum region indicating the limitation of our model.

5.3. Summary

Relationship between size and position of collection structure with the turbulence was established. Turbulence produced in the flow field, increased with the increases in cross sectional area of structure perpendicular to the gas flow. It also increased with the decreases in distance of structure from cylinder wall. Aerodynamic profile of collection structure needed to be improved and shielding baffle should be used to reduce the turbulence in main chamber.

Chapter 6

Effect of Temperature Gradient

To study the effect of cylinder temperature on fluid dynamics and countercurrent, a temperature gradient was applied on cylinder wall. A UDF was written to assign a temperature gradient to cylinder wall. Two cases of different temperature gradient were discussed below.

In first case, 10-degree Kelvin temperature gradient was applied on the cylinder wall. UDF (Appendix-D) assigned a temperature of 300K to cylinder top and 310K to cylinder bottom. Cylinder wall temperature varied linearly from 300K (top side) to 310K (bottom side).

In Second case, 20-degree Kelvin temperature gradient was applied on the cylinder wall. UDF (Appendix-E) assigned a temperature of 300K to cylinder top and 320K to cylinder bottom. Cylinder wall temperature varied linearly from 300K (top side) to 320K (bottom side).

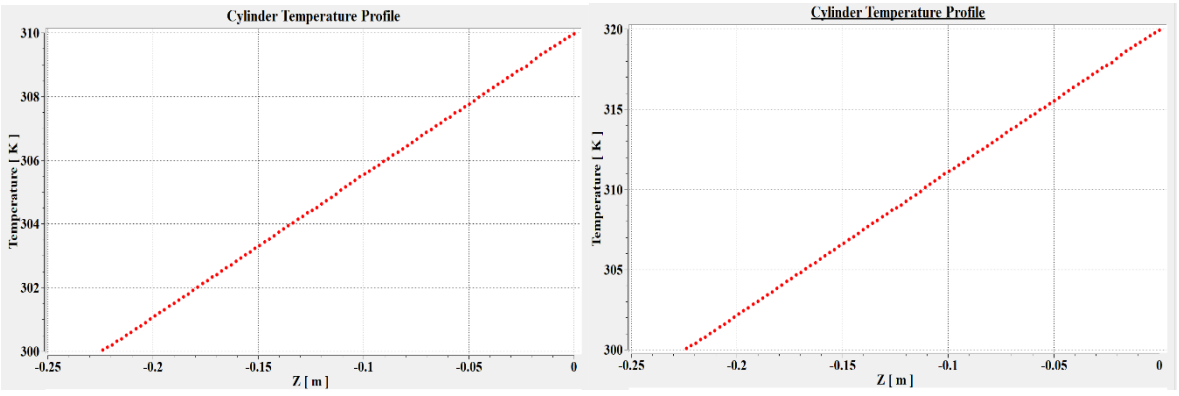

Figure 6.1: Cylinder temperature gradient, a) 10K b) 20K

Flow profile with the axial temperature gradient showed that the energy flux density and axial mass flux density was increased when 10K temperature gradient was applied as compared to 0K gradient. Countercurrent was increased further as the temperature gradient was increased to 20K gradient. Same behavior was observed with two outlets.

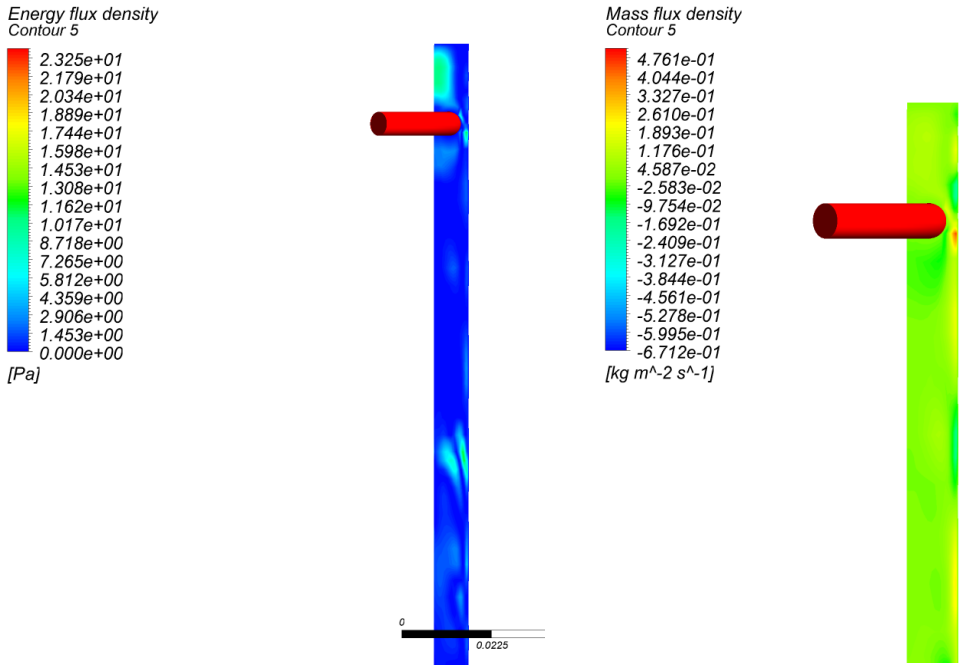

Figure 6.2: Flow Profile with single outlet at 10K temperature gradient, a) Energy Flux Density b) Mass Flux Density

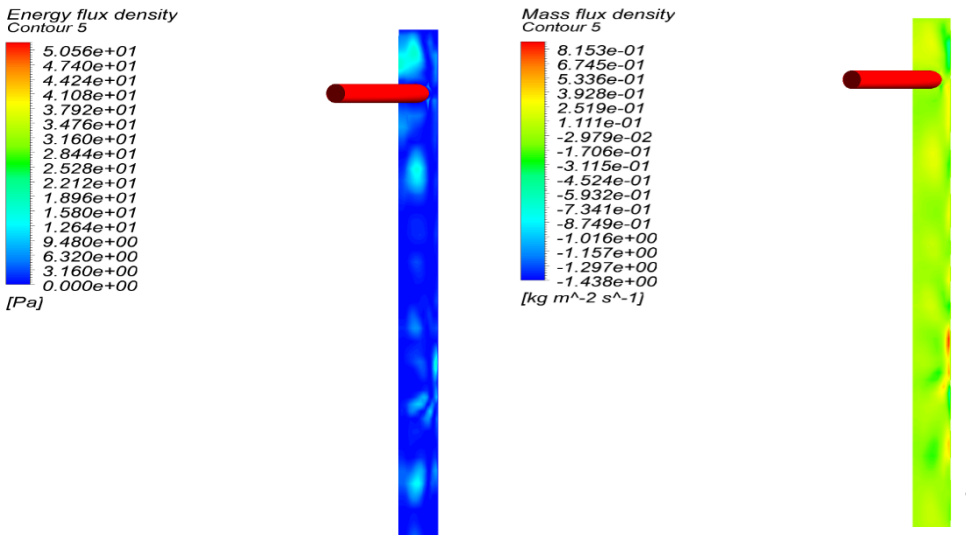

Figure 6.3: Flow Profile with single outlet at 20K temperature gradient, a) Energy Flux Density b) Mass Flux Density

The reason was that particles at high temperature end of cylinder had high kinetic energy and moved toward the cylinder center (Low vacuum region). Once they were at the center, they were sucked towards high vacuum in axial direction and then towards the rotor wall due to centrifugal force, causing a net countercurrent flow.

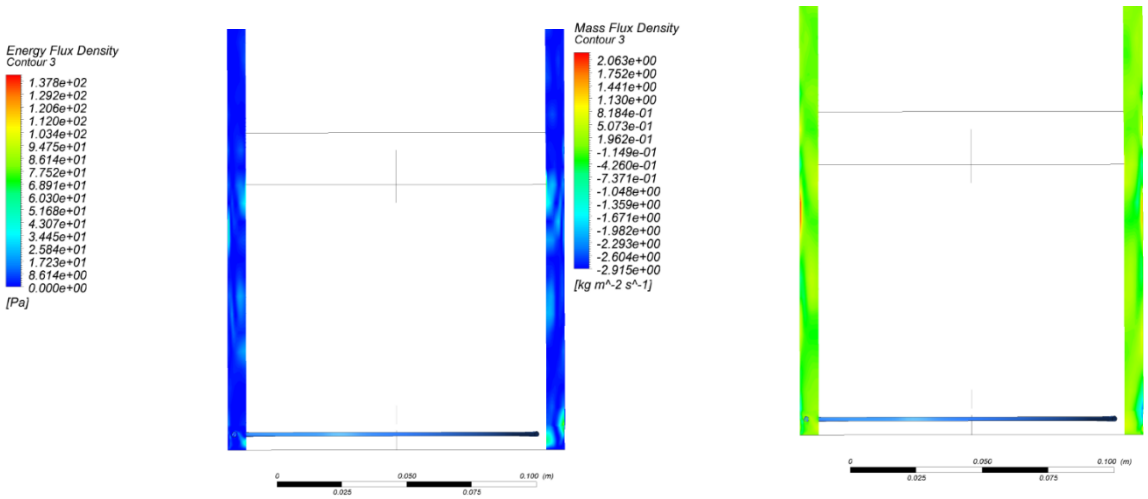

Figure 6.4: Flow Profile with double outlet at 20K temperature gradient, a) Energy Flux Density b) Mass Flux Density

S. V. Bogovalov [1] modeled the effect of countercurrent with 10K temperature gradient in 2D axisymmetric model. He modeled collection structure as pulsed breaking force. Result's pattern in his case were same as ours but values were different as we used 3D structural geometry instead of pulsed breaking force. Our model also encounters the 3D effect of flow which were totally ignored in Bogovalov model.

In actual case temperature gradient is limited by internal mechanical and physical processes and cannot be controlled independently. And structure diameter is optimized with collection stream mass flow and pressure.

6.1. Summary

Effect of temperature gradient on Countercurrent were examined with single and two outlets. It was found that the intensity of countercurrent was increased as the temperature gradient along the cylinder wall was increased. Temperature effect on countercurrent was exaggerated with two outlets because of stronger mechanical drive.

References

[1] F. L. A. M. Thissen, “Equipment for Automatic Optical Inspection of Connecting-Lead Patterns for Integrated Circuits.,” *Philips Tech. Rev.*, vol. 37, no. 4, pp. 77–88, 1977.

Chapter 7

Conclusion and Recommendation

A CFD model was developed to examine the flow regime in rotating cylinder. Turbulence due to collection structures in a rotating cylinder was also investigated. Comparison of our model with other published work was made and following conclusions were drawn,

- Shockwaves were generated due to interaction of fast rotating gas with a stationary structure. Intensity of these waves was directly proportional to the cross-sectional area of structure perpendicular to the gas flow vector and inversely proportional to the distance between the structure and cylinder wall.

- Design of collection structure should be optimized aerodynamically to minimize the drag in gas. Blunt ends needed to be eliminated for smooth flow region.

- Cylinder temperature profile also effected the axial countercurrent. Intensity of countercurrent increased with the increase the axial temperature gradient of cylinder wall.

- S. V. Bogovalov, V. A. Kislov, and I. V. Tronin [1], [2] modeled the collection structures as a source of mass and momentum. They presented two cases, in first they modeled structures as a stationary mass and momentum source while in second they modeled structures as a pulsed breaking momentum source. Our results showed that the spiral shockwaves disturb the pressure at cylinder wall and gas velocity in axial direction as predicted by Bogovalov's model with pulsed breaking force. Stationary source model is unable to predict the waves captured in our case.

- Values predicted by Bogovalov's model for axial velocity are slightly higher as his model did not take account of inlet and outlet flows.

- JIANG Dongjun and ZENG Shi [3] presented a model to predict the generation of shockwaves due to collection structure. He modeled the collection structures as straight pipe extending radially outwards. Our model showed that effect of shockwaves due to circular structure is considerably greater than the radially straight collection structure. The reason is that the circular structure at larger radius presents a very high resistance to flow as compared to an extended tip.

- Presence of shockwave in the rotating cylinder suggested that the limitation on computational domain applied by the knudsen boundary restricted us to comprehensively examine the axial countercurrent flow as molecules of gas were also present in the central high vacuum region.

7.1. Recommendations

- Different designs of collection structure should be explored to minimize the drag in gas flow.

- To completely analyze the axial countercurrent flow particle-based approach (Langrangian approach) should be used.

References

[1] S. V. Bogovalov, V. A. Kislov, and I. V. Tronin, “Waves in a gas centrifuge,” J. Phys. Conf. Ser., vol. 751, no. 1, 2016.

[2] S. V. Bogovalov, V. A. Kislov, and I. V. Tronin, “Impact of the pulsed braking force on the axial circulation in a gas centrifuge,” Appl. Math. Comput., vol. 272, pp. 670–675, 2016.

[3] D. J. Jiang and S. Zeng, “3D numerical study of a feed jet in a rotating flow-field,” J. Phys. Conf. Ser., vol. 751, no. 1, pp. 6–11, 2016.

Publication

Muhammad Zunair, Dr. Majid Ali

"CFD Study of Structurally Induced Turbulence for Compressible Fluid in Rotary Domain"

International Conference on Aerospace Science and Aviation Technology (ICASAT),

Islamabad, Pakistan, 22 - 23 December, 2020

Paper ID: EW-SATISLAM-221220-336

Appendices

Appendix A

Onsager's Master Equation: $\frac{\partial^2}{\partial \xi^2}\left\{e^{\xi}\frac{\partial^2}{\partial \xi^2}\left(e^{\xi}\frac{\partial^2 X}{\partial \xi^2}\right)\right\}+\frac{1+A^2 P_r\frac{\gamma-1}{2\gamma}}{16A^2\epsilon^2\left(\frac{z}{a}\right)^2}\frac{\partial^2 X}{\partial \eta^2}$

Here,

$\xi = A^2\left(1-\frac{r^2}{a^2}\right)$, $\eta = \frac{z}{Z}$, $P_r = \frac{\mu C_p}{kM}$,

$\epsilon = \frac{\mu}{\rho_w \Omega a^2}$, $\frac{4A^2}{a^4}\left(\frac{\partial^2 X}{\partial \xi^2}\right) = P_{eq}W$, $A^2 = \frac{M\Omega^2 a^2}{2RT_o}$,

$P_r = Prandtl\ number$, $\Omega =$ Rotational speed of cylinder,

$\gamma = Ratio\ of\ specific\ heats$,

$\rho_w = Pressure\ at\ wall\ of\ rotating\ cylinder$

$X = Onsager's\ master\ potential\ function$

Appendix B

Mean Free Path Length: $\boldsymbol{\lambda = \frac{M}{\sqrt{2}\pi\sigma^2\rho_o N_{av}}}$

Here

λ = Mean free path length, N_{av} = Avogadro number

σ = Molecular diameter of gas, ρ_o = density of gas

$\rho_o = \rho_w e^{-A^2\left[1-\frac{r^2}{a^2}\right]}$

$A^2 = \frac{M\Omega^2 a^2}{2RT_o}$

Ωa = Peripheral speed

Appendix C

Navier-Stroke's equation in 3D cylindrical coordinate system for steady state is given as follow,

Mass Continuity: $\frac{1}{r}\frac{\partial}{\partial r}(\rho r V_r) + \frac{\partial}{\partial z}(\rho V_z) = 0$

Axial Momentum: $\rho(V_r \frac{\partial V_z}{\partial r} + V_z \frac{\partial V_z}{\partial z} = -\frac{\partial p}{\partial z} + \mu\left\{\frac{1}{r}\frac{\partial}{\partial r}\left(r\frac{\partial V_z}{\partial r}\right) + \frac{\partial^2 V_z}{\partial z^2}\right\} + \rho g$

Radial Momentum: $\rho(V_r \frac{\partial V_r}{\partial r} - \frac{{V_\theta}^2}{r} + V_z \frac{\partial V_r}{\partial z} = -\frac{\partial p}{\partial r} + \mu\left\{\frac{\partial}{\partial r}\left[\frac{1}{r}\frac{\partial}{\partial r}(rV_z)\right] + \frac{\partial^2 V_r}{\partial z^2}\right\}$

Azimuthal Momentum: $\rho(V_r \frac{\partial V_\theta}{\partial r} + \frac{V_r V_\theta}{r} + V_z \frac{\partial V_\theta}{\partial z} = \mu\left\{\frac{\partial}{\partial r}\left[\frac{1}{r}\frac{\partial}{\partial r}(rV_\theta)\right] + \frac{\partial^2 V_\theta}{\partial z^2}\right\}$

Energy Equation: $\rho C_v\left(V_r\frac{\partial T}{\partial r} + V_z\frac{\partial T}{\partial z}\right) + T\left(\frac{\partial p}{\partial T}\right)\left[\frac{1}{r}\frac{\partial}{\partial r}(rV_r) + \frac{\partial V_z}{\partial z}\right] =$

$$k\left[\frac{1}{r}\frac{\partial}{\partial r}\left(r\frac{\partial T}{\partial r}\right) + \frac{\partial^2 T}{\partial z^2}\right]$$

Equation of State: $p = \frac{\rho RT}{M}$

Here,

$r = radius,$ $\rho = Density,$ $T = Temperature,$ $\mu = Viscosity,$

$g = Gravity,$ $k = Thermal\ Conductivity\ of\ gas,$

$C_v = Specific\ heat\ at\ constant\ volume,$

$V_r = Velocity\ component\ in\ radial\ direction,$

$V_z = Velocity\ component\ in\ axial\ direction,$

$V_\theta = Velocity\ component\ in\ azimuthal\ direction$

Appendix D

UDF for single outlet (10K Temperature Gradient) is as follow,

```
/************************************************************************
*******UDF for specifying Temperature gradient profile boundary
profile for a Cylinder Wall
************************************************************************
**/ #include "udf.h"
DEFINE_PROFILE(Temp_profile,t,i)
{
real x[ND_ND];
face_t f;
begin_f_loop(f,t)
{
F_CENTROID(x,f,t);
F_PROFILE(f,t,i) = 300.0+(10.0*(1.0+(x[2]/(0.224))));
}
end_f_loop(f,t)
}
```

UDF for single outlet (20K Temperature Gradient) is as follow,

```
/************************************************************************
*******UDF for specifying Temperature gradient profile boundary
profile for a Cylinder Wall
************************************************************************
**/ #include "udf.h"
DEFINE_PROFILE(Temp_profile,t,i)
{
real x[ND_ND];
face_t f;
begin_f_loop(f,t)
{
F_CENTROID(x,f,t);
F_PROFILE(f,t,i) = 300.0+(20.0*(1.0+(x[2]/(0.224))));
}
end_f_loop(f,t)
}
```

Appendix E

UDF for two outlets (10K Temperature Gradient) is as follow,

```
/************************************************************************
*******UDF for specifying Temperature gradient profile boundary
profile for a Cylinder Wall
************************************************************************
**/ #include "udf.h"
DEFINE_PROFILE(Temp_profile,t,i)
{
real x[ND_ND];
face_t f;
begin_f_loop(f,t)
{
F_CENTROID(x,f,t);
F_PROFILE(f,t,i) = 300.0+(10.0*(1.0+(x[0]/(0.224))));
}
end_f_loop(f,t)
}
```

UDF for two outlets (20K Temperature Gradient) is as follow,

```
/*************************************************************************
*******UDF for specifying Temperature gradient profile boundary
profile for a Cylinder Wall
*************************************************************************
**/ #include "udf.h"
DEFINE_PROFILE(Temp_profile,t,i)
{
real x[ND_ND];
face_t f;
begin_f_loop(f,t)
{
F_CENTROID(x,f,t);
F_PROFILE(f,t,i) = 300.0+(20.0*(1.0+(x[2]/(0.224))));
}
end_f_loop(f,t)
}
```